DIII-D High Field Side Lower Hybrid Current Drive: Experiment Overview

S.J. Wukitch[1], A. Seltzman[1], S. Shiraiwa[1], P.T. Bonoli[1], Y. Lin[1], C. Holcomb[2], R.I. Pinsker[3]

[1] *MIT Plasma Science and Fusion Center, Cambridge, USA*

[2] *Lawrence Livermore National Laboratory, Livermore, USA*

[3] *General Atomics, La Jolla, CA USA*

Efficient off-axis current drive (OACD) scalable to reactors is a key enabling technology for economical, steady state tokamak. High field side lower hybrid current drive (HFS LHCD) has potential to provide efficient OACD consistent with advanced tokamak (AT) scenarios.[1] In DIII-D, a broad current profile is required for "high q_{min}" and advanced tokamak scenarios.[2] In these discharges, we seek external current drive peaked $0.6<\rho<0.9$ with a current density ~0.4 MA/m^2 for current profile control. For DIII-D AT and scenario development research, magnetic fields down to 1.6 T with central densities approaching 1x10^{20} m^{-3} are expected.[3] With low field side placement of the LHCD launcher, poor wave accessibility and penetration hinder LHCD utilization in DIII-D AT discharges. For HFS LHCD, wave accessibility and penetration are greatly improved as shown in Figure 1. The color scale represents the power remaining in the ray where red is 100% and blue approaching zero. Good penetration is where the ray rapidly penetrates to the region of interest with little absorption and is rapidly absorbed in a single pass. The rays from the HFS demonstrate this. The HFS rays remain red while penetrating into the core and are strongly absorbed where the rays rapidly turns blue. Rays launched from the LFS fail to penetrate the plasma, bounce in the edge and SOL and are absorbed along the ray. On the HFS side, the higher local magnetic field improves wave accessibility ($n_{||acc}\sim\sqrt{n_e}/B$)[4] for low $n_{||}$ which improves wave penetration ($n_{||abs}\sim\sqrt{30/T_e}$) [5]. The current drive efficiency ($\propto 1/n_{||}^2$) [6] also improves dramatically as $n_{||}$ is decreased.

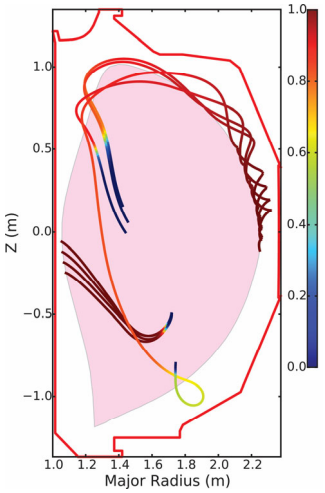

Figure 1: Good wave penetration and single pass absorption for HFS LHCD for waves with $n_{||}$=-2.7 in DIII-D AT discharge (147634). Waves launched from the low field side fail to penetrate.

Due to the quiescent HFS scrape off layer, HFS LHCD has potentially dramatically reduced plasma material interaction (PMI) issues and improved coupling.[1] DIII-D AT discharges provide an opportunity to validate HFS RF wave physics and LHCD physics models.

Additionally, this experiment provides an opportunity to assess whether locating the LHCD coupler on the HFS mitigates coupling and PMI challenges.

To achieve the project's physics mission, a compact coupler adapting proven LHCD coupler technology has been designed where the expected power density is ~32 MW/m^2.[7] To distribute power poloidally, the coupler utilizes a traveling wave poloidal splitter, similar to C-Mod LH coupler.[8] A multi-junction [9] distributes power toroidally and determines the coupler spectrum. The launched spectrum is peaked at $n_{||}$ =-2.7 with a primary reverse spectrum peak at $n_{||}$ =+8.1. Simulations including the reverse spectrum for an AT discharge (147634, B_T=1.66 T) shows that the reverse peak generates no significant current and the net current is ~140 kA. In this simulation, ~1 MW out of 1.6 MW launched is coupled to $n_{||}$ =-2.7, consistent with the expected coupler spectrum. An alternative design using a wider aperture was considered but had significant reverse spectrum power that drove ~30 kA, resulted in a wider coupler, and had lower directivity.[7]

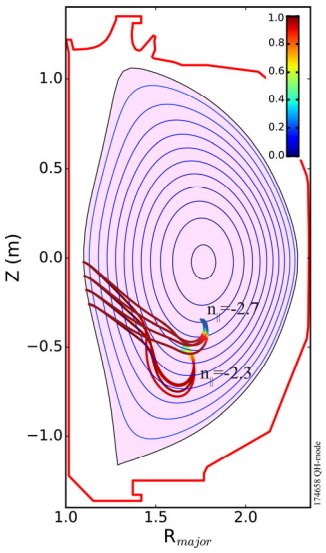

Figure 2: Wave propagation and absorption differs for $n_{||}$=-2.3 than for $n_{||}$=-2.7 which will allow for model validation.

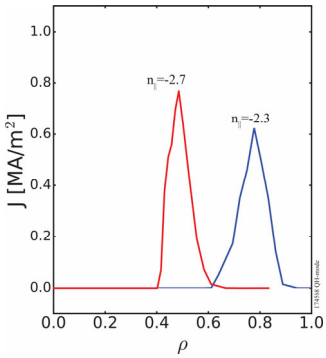

Figure 3: LH wave deposition and resulting driven current profile is sensitive to launch $n_{||}$.

To validate the HFS LHCD wave propagation and absorption, we take advantage of the flexible coupler $n_{||}$ spectrum and higher where the wave accessibility is improved. The coupler peak $n_{||}$ spectrum can be varied from ~2.2-3.4 at the expense of directivity [7] and higher B_T discharges, specifically B_T>1.8 T, allows for lower access $n_{||}$. For discharge 174658 (QH-mode, B_T~2 T), two $n_{||}$ have different wave penetration and driven current profiles, see Figure 2. The higher $n_{||}$ propagate to smaller radius while the low $n_{||}$ drives a current profile peaked farther off axis. The driven current reaches ~240 kA and current density in excess of the required 0.4 MA/m^2. To utilize QH-mode discharges, QH-mode operation would need to be extended to B_T+ and I_P+ configuration.

From simulations of existing discharges, wave penetration was found to be most sensitive to edge q profile. For high edge q (q_{edge}>8) discharges, the wave propagates into the plasma center but mode converts to the fast wave and propagates back to the plasma edge. Artificially lowering the q_{edge}, the wave penetrates and damps. The origin of the poor penetration and

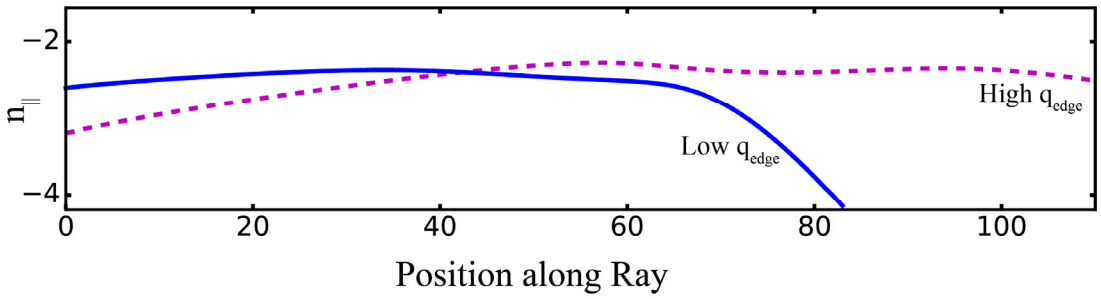

Figure 4: Scenarios with good wave penetration, the $n_{||}$ downshift is balanced by poloidal upshift and $n_{||}$ remains constant until rapid poloidal upshift and absorption.

absorption is a result of $n_{||}$ downshift along the ray. As shown in Figure 4, $n_{||}$ is significantly down shifted for the high q_{edge} discharge. In the low q_{edge} (q_{edge}<8) discharges, the poloidal induced $n_{||}$ upshift balances the 1/R toroidal downshift and $n_{||}$~constant. In future experiments, scan of edge q or plasma current could be used to validate simulations.

To accommodate a HFS LHCD coupler in DIII-D, several technical challenges had to be overcome. Foremost was to minimize the impact on the in-vessel components both in operation and during installation. As shown in the in-vessel schematic, the top of the coupler is at the mid-plane and runs down the center post under the tiles. The waveguide exit under the divertor floor tiles, divertor shelf, cryopump, baffle plate and outer wall tiles before exiting out the port. On the center post, the tile thickness is planned to be increased by ~2.5 cm to accommodate the HFS launcher over a limited region. Two toroidal bands of increased tile thickness are planned at the coupler and the lower tiles. In addition, vertical columns of tiles on either side of the center post waveguides between the two toroidal bands so called ribs will also have increased tile thickness. Additional "ribs" will be placed symmetrically about the machine at two to three locations based on thermal considerations. On the vessel floor, the primary governing constraint were the supports for the divertor shelf and divertor floor tile height. Moving or changing the supports would require lifting the shelf and would be costly in time and resources. The waveguide under the divertor floor tiles and divertor shelf is WR-159 and run radially in pairs under the floor tiles. To accommodate the waveguide pairs, the floor tile channel width is increased ~2.8 cm while maintaining ~1 cm radius for the channel. Thermal analysis of the modified tiles shows that proposed tiles have similar stress as the current tiles. The waveguide avoids the cryopump supports but the baffle plate supports will need to be modified. The limited space also required limited flanges inside the DIII-D vacuum vessel and there are two: one at the 45 deg tile and the other just above the cryopump. Thus, each submodule is composed of three waveguide sections. The flanges are a low profile flange adapting a conflat and RF joint for both a vacuum and RF seal. A prototype has successfully undergone a series of 80 one

hour, 400°C bake cycles and ten 16-hour, 400°C bake cycles. The concern was that the copper gasket would anneal during the machine bake and fail to hold vacuum. The prototype test is equivalent to 5 years of bake cycles and two years of bake time. To minimize return loss, we use six mitre bends per submodule and the estimated return loss is -29 dB. The calculated resistive loss is -0.55 dB using the measured conductivity of the sample waveguide.

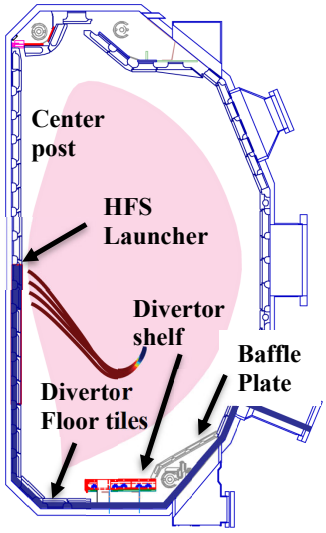

Figure 5: HFS LHCD waveguide from coupler to vacuum flange will run under the center post and divertor floor tiles, divertor shelf and cryopump.

For the coupler and in-vessel waveguide, copper cannot be utilized as structural material due to the 380°C machine bake (anneals copper) and disruption loads. We have explored a newly developed copper alloy, GRCop-84, that retains good strength at 400°C and higher.[10] Additive manufacturing limits individual component length <40 cm[11]. The plan is to utilize, AM GRCop-84 for the center post waveguide and coupler. With minimal post processing, a surface finish consistent with high power operation appears obtainable. To assemble AM pieces, we have explored electron beam and laser welding. An important observation is that the niobium chromate in GRCop-84 aggregates and precipitates out if excess heat and time is used in the welding process. The coupler module prototypes are being manufactured and first operation is planned for FY2021.

Work supported by the U.S. DoE, Office of Science, Office of Fusion Energy Sciences, using User Facility DIII-D, DE-FC02-04ER54698, and by Scientific Discovery through Advanced Computing Initiative, DE-FC02-01ER54648.

[1] P.T. Bonoli, et al, Nucl. Fusion 58, 126032, (2018)

[2] C. T. Holcomb, J. R. Ferron, T. C. Luce, T. W. Petrie, et al. Nuclear Fusion **54**, 093009 (2014).

[3] T. C. Luce et al., Fusion Sci. Tech. **48**, 1212–1225 (2005).

[4] M. Brambilla, Nucl. Fusion **19**, 1357 (1979).

[5] Y. Peysson and Tore Supra Team, Nuclear Fusion **41**, 1703 (2001). doi:10.1088/0029-5515/41/11/320.

[6] N. J. Fisch, Phys. Rev. Lett. **41**, 873 (1978).

[7] A. Seltzman, S. Shiraiwa, G.M. Wallace, and S.J. Wukitch, Nucl. Fusion, doi: 10.1088/1741-4326/ab22c8.

[8] S. Shiraiwa et al., Nucl. Fusion, vol. 51, no. 10, p. 103024, Oct. 2011.

[9] L. Delpech et al., Nucl. Fusion **54**, 103004 (2014).

[10] D. L. Ellis and D. Keller, https://ntrs.nasa.gov/archive/nasa/casi.ntrs.nasa.gov/20000064095.pdf.

[11] C. Hayes, E. Brown, and B. Kappes, "Characterization of Selective Laser Melted GRCop-84," in 2018 Joint Propulsion Conference, American Institute of Aeronautics and Astronautics.